Formosa Journal of Applied Sciences (FJAS)
Vol.1, No. 3 2022: 165-176

Novel Direct Downhole Enthalpy Estimation at Geothermal Well in Cubadak, West Sumatra, Indonesia

Anggoro Wisaksono
President University

ABSTRACT: Temperature, pressure and enthalpy data are very important and valuable, both during geothermal drilling and in well operation. Fibre optic distributed temperature sensors (DTS) that offer flexible and robust solutions for geothermal applications and temperature logging, an established method for well temperature measurement. All temperature measurement methods will be combined with reservoir enthalpy estimation using T-p-x state space correlation for H_2O-NaCl geothermal brine. A geothermal brine enthalpy estimation model has been developed, based on T-p-x state space correlation using C programming language. This was able to provide estimations of pressure, mass fraction, density and enthalpy, solely based on measured temperature limited to below 300^oC. The model can be applied to various geothermal fields with sodium chloride dominated waters. The study treated the mixture of geothermal brine and drilling fluid heated in the well for certain periods as a simulation of geothermal brine at the reservoir. The enthalpy monitoring graph proved useful for monitoring the enthalpy in the reservoir. The results from the model are used for early electrical power estimations of the Cubadak geothermal working area site, based on current geothermal gradient extrapolation of CBD-1 well.

Keywords: Geothermal Energy, Geothermal Exploration, Distributed Temperature Sensing, Enthalpy, Hydrothermal, Geothermal Fluid

Submitted: 01-08-2022; Revised: 08-08-2022; Accepted: 16-08-2022

Corresponding Author: anggoro@president.ac.id

INTRODUCTION

During exploration drilling activity, the high temperature fluid in geothermal reservoir is a hostile environment for downhole tools. Drilling mechanisms in geothermal energy are therefore not the same as for oil and gas (Blankenship & Finger, 2010). Since the depth of the boreholes are deeper, the downhole tools have to be resistant to a relatively a high temperature environment. The more advanced geothermal fields in certain location have been taken as conceptual models in reservoir, but attempts to apply these models in different environmental and geological settings generate ambiguous results (Younger, 2014). Therefore, better understanding of these resource systems in various environments are needed, especially for geothermal exploration risk mitigation.

Attempts and experiments have been conducted to overcome the above exploration challenges. One of the examples is using the high temperature resistant DTS (Distributed Temperature Sensing), which is fibre optic photon counting distributed temperature measurement technology for borehole temperature measurement. This direct measurement technique, incorporated with distributed enthalpy estimation, resulted in direct non-calibrated estimation, along with the distributed temperature measurement.

GEOTHERMAL SITE OVERVIEW

The Cubadak geothermal site in West Sumatra province is located around the famous Cubadak water spring, with a total area of 20 km^2. Based on the geological description from government investigations (Coal Mineral and Geothermal Resources Centre (PSDG), 2018),

One surface manifestation is the Sawah Mudik hot spring in Betung village. Water samples taken from Sawah Mudik are from 37.1 to 74.8^oC with a neutral pH of 6.35-6.84 (Ministry of Energy and Mineral Resources (ESDM), 2017). The water is mixed between chloride and bi-carbonate waters. According to Na-K geothermometry, the reservoir temperature is probably 235^oC (Ministry of Energy and Mineral Resources (ESDM), 2017). One geothermal well has been drilled during the most recent exploration, which is CBD-1.

METODOLOGY

In hydrothermal reservoirs that produce two phase fluids, it is important to monitor the enthalpy trends of the fluids in order to monitor performance of the well (Hirtz, Lovekin, Copp, Buck, & Adams, 1993) (Spielman, 2003) (Juliusson, 2006). For instance, decreasing enthalpies may indicate breakthrough of injection water or intrusion of cooler groundwater. Conversely, increasing enthalpies may indicate reservoir boiling and the formation of a steam cap (Hirtz,

Lovekin, Copp, Buck, & Adams, 1993). Enthalpy is also essential to interpret geochemical data, to determine the steam fraction and to allow for the correction of chemical concentrations back to reservoir conditions (Atalay, 2008). From an operational point of view, the enthalpy and the mass flowrate indicate the amount of steam available and, most importantly, the power output of the plant (Atalay, 2008).

Temperature data is a key parameter and can be utilised for enthalpy estimation in geothermal applications according to the literature (Grant, 2015) (Hyndman, Davis, & Wright, 1979). Therefore, this study indicated the possibility of reliably estimating the enthalpy from a measured temperature taken directly from a borehole without analysing the liquid at the surface. The previous laboratory experiment by Wisaksono et. al. of estimating the enthalpy from a measured temperature using fibre optic Raman scattered photon counting distributed temperature measurement has been published in the conference proceedings of 42th Stanford Geothermal Workshop 2017, and in 5th Indonesia International Geothermal Conference and Exhibition 2017 (Wisaksono, Pizzone, Gemmell, Younger, & Hadfield, 2017) (Wisaksono, Experimental study of fibre optic photon counting application: Real time-free calibration distributed temperature measurement and enthalpy estimation for geothermal well, 2017).

Distributed temperature sensing (DTS)

The concept is based on photon counting measurements of Raman backscatter. This was to extend the range of the system from the previous study by increasing the optical power and reducing the repetition rate of the excitation laser (Wisaksono, Pizzone, Gemmell, Younger, & Hadfield, 2017).

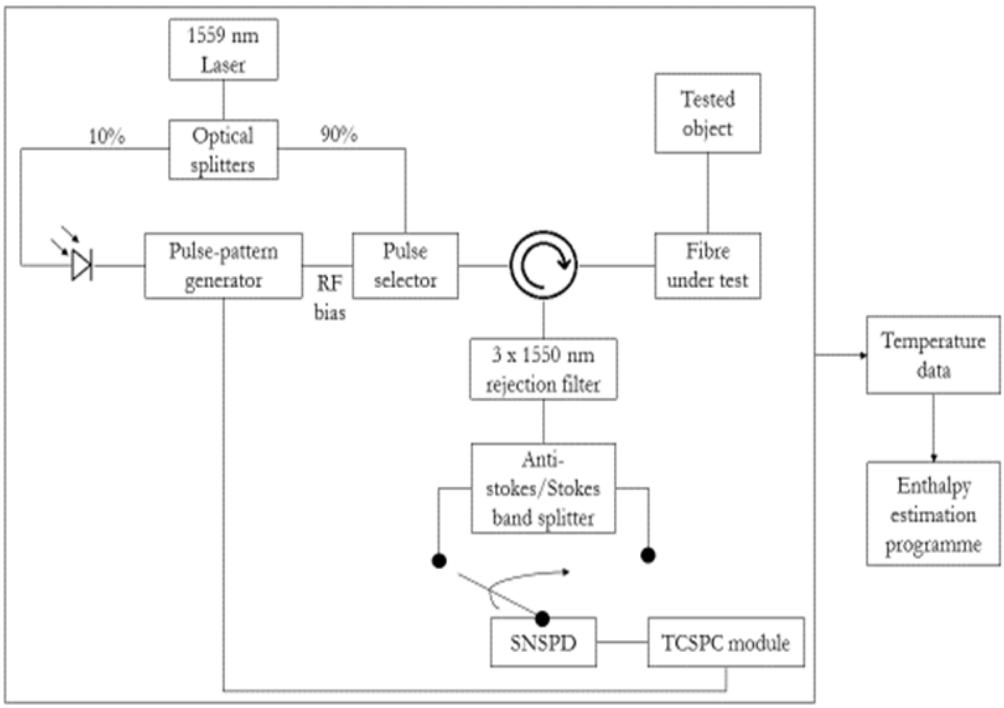

Figure 1. System diagram of the Raman backscattered temperature sensor

The light that is backscattered from the FUT is directed by the circulator to three 1550nm filters installed between the circulator and anti-stokes/stokes band splitter in order to reject Rayleigh photons around the 1560 nm wavelength, to gain Raman photon only. Before the backscattered light reaches the photon detector, it will go through a final splitter, which separates the Stokes and anti-Stokes signals. The detector selected for this temperature sensing is a superconducting nanowire single-photon detector (SNSPD), used as the photon detector.

Figure 2. Flow chart of a fibre temperature sensor based on Raman backscattering. Stokes and anti-Stokes signals are collected to be modelled to get the distributed temperature data.

The temperature $T(y)$, where is the temperature at each fibre position y, can be extracted using equation 1. $\hbar$ is the reduced Planck constant, F_{as_p} is the frequency shift between anti-Stokes peak and pump peak, I'_s and I'_{as} are backscattered Stokes and anti-Stokes photons per second respectively and k_B is the Boltzmann constant:

$$T(y) = \frac{\hbar|F_{as\_p}|}{k_B ln\left(R_{gr}\frac{II_S(x)-B_S}{II_{as}(x)-B_{as}}\right)} \ldots\ldots\ldots\ldots\ldots (1)$$

The temperature readings can then use as inputs to the geothermal brine model application to get the thermodynamic data for the fluid and then for the range of geothermal brine mixtures using $T-p-x$ state space correlation model for H_2O-NaCl geothermal brine developed by Palisser and McKibbin (Dreisner, 2007) (Driesner & Heinrich, 2007) (Mantegazzi, Sanchez-Valle, & Dreisner, 2013). This was able to provide estimations of pressure, mass fraction, density and enthalpy, solely based on measured temperature limited to below 300°C. The model can be applied to various geothermal fields with sodium chloride dominated waters.

Direct downhole enthalpy estimation

In this study, we will try to obtain the result by direct estimates, when fibre optic cable was inside the well measuring downhole or reservoir temperature. Wahl (Wahl, 1977) has determined a method to estimate the sodium chloride brine. The heat capacity of sodium chloride is 0.2 compared to water which is 1, in which case from Na/K geothermometry analysis (Wahl, 1977), the heat capacity C_B will be:

$$C_B = \left[C_w\left(1-\frac{w_t}{100}\right) + (0.002+B)w_t\right] \ldots\ldots\ldots\ldots\ldots (2)$$

In this formula, C_w is water heat capacity, w_t is weight concentration of total dissolved solids (TDS) and using B as arbitrary constant. From here, enthalpy (h) of the brine mixture can be calculated from the foregoing information by integrating brine heat capacity (C_B) over the given temperature range from T_0 and T to:

$$h = \int_{T_0}^{T} C_B dT \ldots\ldots\ldots\ldots\ldots (3)$$

so that the formula will be:

$$h = \int_{T_0}^{T}\left[C_w\left(1-\frac{w_t}{100}\right) + (0.002+b)w_t\right] dT \ldots\ldots\ldots\ldots\ldots (4)$$

For two-phase liquid and vapour sodium chloride waters, $T-p-x$state space correlation model for estimating the properties in H_2O–NaCl geothermal brine, starting from pressure p_{brine} , for temperature T<300°C (Palliser & McKibbin, A Model for Deep Geothermal Brines, I: T-p-X State-Space Description, 1998):

$$p_{brine}(T) = a_1 t + a_2 t^2 + a_3 t^3 + a_4 t^4 + a_5 t^5 \ldots\ldots\ldots\ldots\ldots (5)$$

And then the estimated liquid density ρ_{liq_sat} and vapour density ρ_{vap_sat} for saturated liquid geothermal brine when temperature ≤ 374°C (Palliser &

McKibbin, A Model for Deep Geothermal Brines, II: Thermodynamic Properties – Density, 1998) are:

$$\rho_{liq\_sat}(T) = f_0 + f_1 t + f_2 t^2 + f_3 t^3 + f_4 T^4 + f_5 T^5 + f_6 T^6 \ldots\ldots\ldots\ldots (6)$$

$$\rho_{vap\_sat}(T) = g_1 t^2 + g_2 t^4 + g_3 T^6 + g_4 T^8 + g_5 T^{10} \ldots\ldots\ldots\ldots (7)$$

The formula for the mass fraction in two phase liquid boundary flow for both vapour x_{v2p} and liquid x_{l2p} at temperature ≤374.15°C (Palliser & McKibbin, A Model for Deep Geothermal Brines, I: T-p-X State-Space Description, 1998), are:

$$x_{v2p}(T,p) = x_{vap\_sat}\left[\frac{p_w - p}{p_w - p_{brine}}\right]^z \ldots\ldots\ldots\ldots (8)$$

$$x_{l2p}(T,p) = x_{liq\_sat}\left[\frac{p_w - p}{p_w - p_{brine}}\right]^z \ldots\ldots\ldots\ldots (9)$$

Finally, the brine enthalpy in two phase flow brine enthalpy for both liquid h_{l2p} phase at T≤374.15°C for the fluid (Palliser & McKibbin, A Model for Deep Geothermal Brines, III: Thermodynamic Properties – Enthalpy and Viscosity, 1998):

$$h_{l2p}(T,p) = h_{liq\_sat} + \left[h_w - h_{liq\_sat}\right]\left[\frac{p_w - p}{p_w - p_{brine}}\right]^{\frac{1}{1.4}} \ldots\ldots\ldots\ldots (7)$$

And for the brine phase flow brine vapour enthalpy h_{v2p}, for T≤374.15°C (Palliser & McKibbin, A Model for Deep Geothermal Brines, III: Thermodynamic Properties – Enthalpy and Viscosity, 1998):

$$h_{v2p}(T,p) = h_{vap\_sat} + \left[h_{vap\_w} - h_{vap\_sat}\right]\left[\frac{p_w - p}{p_w - p_{brine}}\right]^{\frac{1}{1.7}} \ldots\ldots\ldots\ldots (8)$$

Pitzer et al. model for H_2O–NaCl covers brine temperatures up to 300°C at various pressures. There are also enthalpy tables in which the pressure has been set to 200, 400, 600, 800 and 1000 bar with temperatures in the range 0-300°C (Pitzer, Piper, & Busey, 1984). On the other hand, latest thermodynamic formulation for H_2O-NaCl by Dreisner (Dreisner, 2007) has been published recently for temperatures up to 800°C and pressures up to 45000 bar. Both models by Pitzer et al. and Dreisner will be used in this study as comparison.

.

RESULTS AND ANALYSIS

The study was focusses on a geothermal well in Cubadak geothermal working area, which is CBD-1 well. Direct measurement in the was field preferred, but due to Covid-19 pandemic, was not possible. Since initial temperature data have been obtained from literature published by Indonesian Geological Agency (Badan Geologi) (Coal Mineral and Geothermal Resources Centre (PSDG), 2018), we decided to use it as the model source of data. And we assumed that the data were measured using DTS.

The available temperature data, were logging data for geothermal gradient (distributed), hence can be used to simulate output of measurement from DTS for $T - p - x$ state space correlation model.

Enthalpy estimation analysis

CBD-1 was drilled to a depth of 703.9 m. The surface temperature T_0 was 22.27°C, with a maximum temperature of 68.89°C at 700 m. The drilling fluid equilibrated in the well for 40 hours. The temperature measurement when the probe lifted (T_1) was 72.9°C at 700 m and 26.75°C at the surface. The temperature anomaly started at 410 m depth (see figure 3). As reported in the government field report investigation, fractures were found at this depth after the clay cap, where the lost circulation of 40-60 l/minute drilling fluid occurred during drilling. The fractures consist of secondary quartz and andesite fragments (probably structure zone) (Coal Mineral and Geothermal Resources Centre (PSDG), 2018) (Ministry of Energy and Mineral Resources (ESDM), 2017). According to this, the study assumed 410 m as the top surface of the reservoir for the enthalpy estimation modelling.

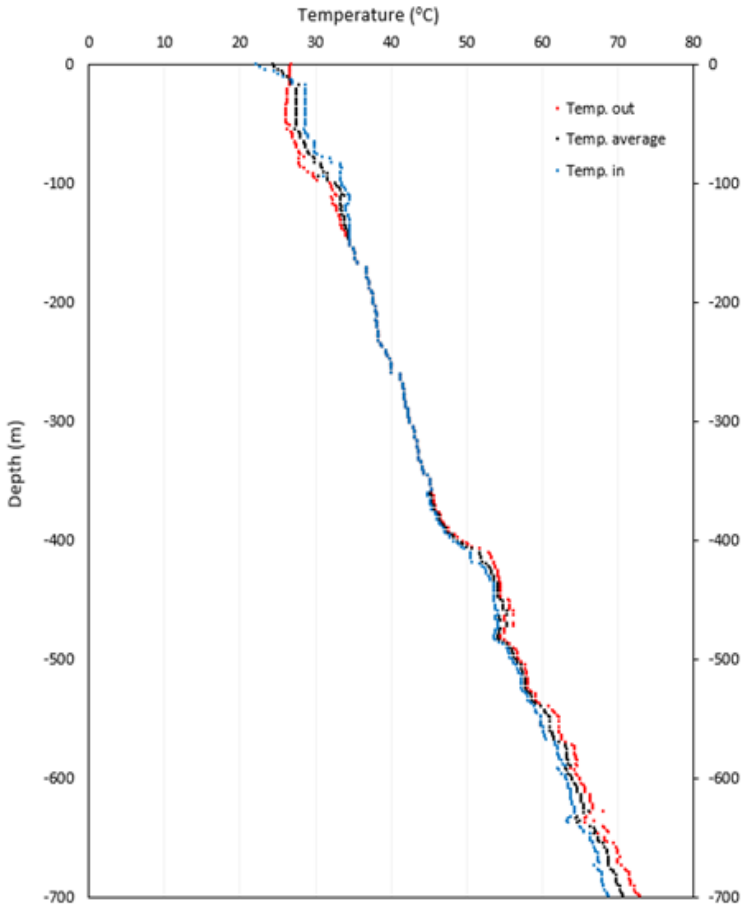

Figure 3. Distributed temperature logging of CBD-1 well

Using average well temperature data, Table 1 shows the fluid, vapour and two phase enthalpy estimations according to the model from 410 m and 700 m depth. Figure 4 shows the enthalpy monitoring simulation for well CBD-1, using equations in section III.B. These equations are also used for the reservoir enthalpy monitoring graph in figure 4. The monitoring shows enthalpy estimations from 410 m to 700 m.

Table 1. Enthalpy estimation at temperature anomaly and well bottom

Depth (m)	T_{avg} (°C)	h_{liq_sat} (kJ/kg)	h_{vap_sat} (kJ/kg)	h_{l2p} (kJ/kg)
410	51.73	163.83	2627.47	823.34
700	70.90	213.98	2665.3	878.77

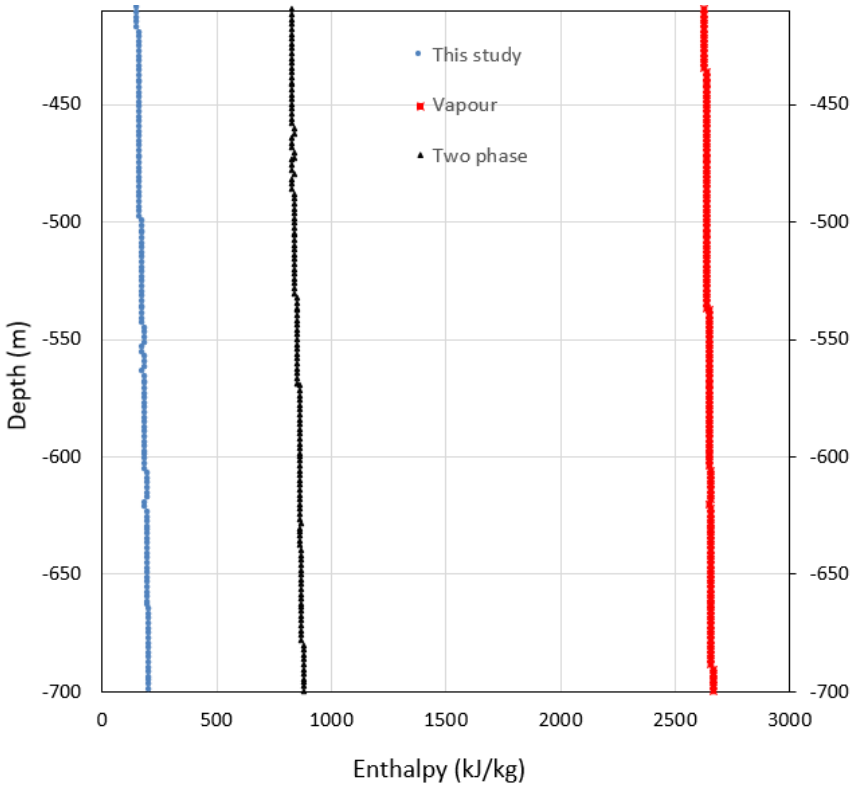

Figure 4. Downhole enthalpy monitoring at well CBD-1.

Meanwhile, Figure 5 compares the study results with other H_20-NaCl fluid formulations. The brine fluid enthalpy plot of this study are aligned and lower when compared with Pitzer et al. (Pitzer, Piper, & Busey, 1984) whose results followed those of Driesner (Dreisner, 2007) at 500-504 m, since these were

constant to a 600 m reservoir depth. These studies used different constants according to the different liquid samples, leading to these distinctions.

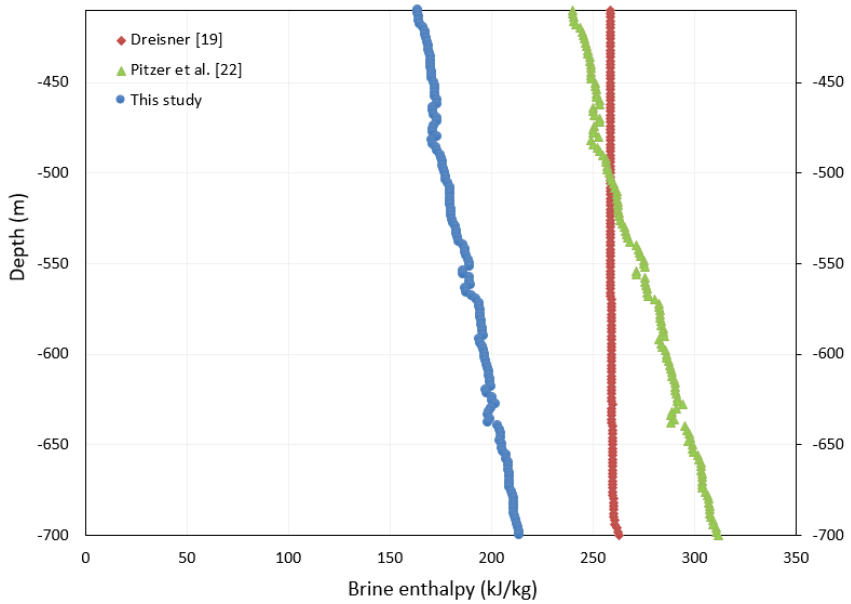

Figure 5. Well CBD-1 enthalpy estimation result compared to other models

Using the constants in the volumetric equation table and data from the model in table II, the estimated potential power (P_{rv}) would be 3.65 MW. In production, the estimated electricity power (P_E) from well CBD-1 alone at 500 m would be 36.57 MWe. The result may still not be sufficient for electricity production for West Sumatra provincial demand. However, according to surface manifestation analysis and the temperature build-up in this well, a deeper well is needed to reach the high enthalpy reservoir.

Table 2. Enthalpy estimation at temperature anomaly summary

	T_0 68.89°C	T_1 72.9°C
h_{liq_sat} (kJ/kg)	209.01	218.92
x_{liq_sat}	0.2708	0.2716
ρ_{liq_sat} (kg/m^3)	1533.72	1544.16
h_{vap_sat} (kJ/kg)	2661.57	2669.00
x_{vap_sat}	0.0013	0.0013
ρ_{vap_sat} (kg/m^3)	5.419	5.633

CONCLUSION

The research was then able to create a simulation combining temperature logging and the enthalpy estimation model, using real temperature logging data. Thus, it has been possible to simulate the mixture of geothermal brine and the drilling fluid that is equilibrated in the well and is at the same temperature as the geothermal brine in the reservoir. The model developed has produce three results for each geothermal well; temperature logging graph, enthalpy monitoring graph and the enthalpy estimation plots with brine mass fractions.

The extrapolated geothermal gradients show that the well needs to be extended to 2865 m to reach a reservoir temperature of 235^{o}C. The potential electricity at this depth is estimated to be 173.48 MWe, which is a very good prospect that could add to the current electrification ratio of 87.55%. The current geothermal energy development strategy of Sarulla (3x110 MWe) in neighbouring province of North Sumatra is an excellent example for future development of the Cubadak geothermal area.

ADVANCE RESEARCH

Although the study are still ongoing at the time of writing, initial findings indicate the hypothesis of the real time pressure and enthalpy reporting model,, from direct and free calibration downhole measurement of temperature.

Following the current result, the study's future aim is to test the tool in one of the geothermal boreholes in Indonesia, to test the efficacy of the real-time pressure and enthalpy model, based on temperature sensing results, up to 1-1-5 Km depth and initially over the temperature interval 100-200^{0} C.

REFERENCES

Atalay, N. (2008). *Downhole Enthalpy Measurement in Geothermal Wells with Fiber Optics.* Stanford: Stanford Geothermal Program, Interdisciplinary Research in Engineering and Earth Sciences.

Blankenship, D., & Finger, J. (2010). *Handbook of Best Practices for Geothermal Drilling.* Albuquerque: Sandia National Laboratories.

Coal Mineral and Geothermal Resources Centre (PSDG). (2018). *Well CBD-1 log data.* Bandung: Coal Mineral and Geothermal Resources Centre (PSDG).

Dreisner, T. (2007). The system H2O–NaCl. Part I: Correlations for molar volume, enthalpy, and isobaric heat capacity from 0 to 1000 °C, 1 to 5000 bar, and 0 to 1 XNaCl. *Geochimica et Cosmochimica Acta, 71*(20), 4902-4919.

Driesner, T., & Heinrich, C. A. (2007). The system H2O–NaCl. Part II: Correlation formulae for phase relations in temperature–pressure–composition space from 0 to 1000 °C, 0 to 5000 bar, and 0 to 1 XNaCl. *Geochimica et Cosmochimica Acta, 71*(20), 4880-4901.

Grant, M. A. (2015). *Geothermal reservoir engineering* (1–12 ed.). John Wiley & Sons, Ltd.

Hirtz, P., Lovekin, J., Copp, J., Buck, C., & Adams, M. (1993). Enthalpy and mass flowrate measurements for two-phase geothermal production by tracer dilution techniques. Stanford: Stanford University.

Hyndman, R. D., Davis, E. E., & Wright, J. A. (1979). The measurement of marine geothermal heat flow by a multipenetration probe with digital acoustic telemetry and insitu thermal conductivity. *Marine Geophysical Research, 4*(2), 181-205.

Juliusson, E. (2006). *An Investigation of Void fraction and Dispersed-Phase Velocity Measurement Techniques.* Stanford: Stanford University.

Mantegazzi, D., Sanchez-Valle, C., & Dreisner, T. (2013). Thermodynamic properties of aqueous NaCl solutions to 1073 K and 435 GPa, and implications for dehyration reactions in subducting slabs. *Geochimica et Cosmochimica Acta, 121*, 263-290.

Ministry of Energy and Mineral Resources (ESDM). (2017). *Indonesia geothermal energy potential chapter 1.* Jakarta: ESDM Geothermal Directorate.

Palliser, C., & McKibbin, R. (1998). A Model for Deep Geothermal Brines, I: T-p-X State-Space Description. *Transport in Porous Media, 33*, 65–80.

Palliser, C., & McKibbin, R. (1998). A Model for Deep Geothermal Brines, II: Thermodynamic Properties – Density. *Transport in Porous Media, 33*, 129-154.

Palliser, C., & McKibbin, R. (1998). A Model for Deep Geothermal Brines, III: Thermodynamic Properties – Enthalpy and Viscosity. *Transport in Porous Media, 33*, 155-171.

Pitzer, K. S., Piper, C., & Busey, R. (1984). Thermodynamic properties of aqueous sodium chloride solutions. *Journal of Chemistry and Reference Data, 13*(1), 1-102.

Spielman, P. (2003, October 12-15). Continuous Enthalpy Measurement of Two-Phase Flow from a Geothermal Well. *Geothermal Resource Council Transactions*, pp. 413-416.

Wahl, E. F. (1977). Hydrothermal Transport of Geothermal Energy. In *Geothermal Energy Utilization* (pp. 13-23). Toronto: John Wiley and Sons.

Wisaksono, A. (2017). Experimental study of fibre optic photon counting application: Real time-free calibration distributed temperature measurement and enthalpy estimation for geothermal well. *Proceedings The 5th Indonesia International Geothermal Convention & Exhibition (IIGCE)* (pp. 1-4). Jakarta: IGA.

Wisaksono, A., Pizzone, A., Gemmell, N. R., Younger, P. L., & Hadfield, R. H. (2017). Direct Downhole Temperature Measurement and Real Time Pressure-Enthalpy Model Through Photon Counting Fibre Optic Temperature Sensing. *PROCEEDINGS, 42nd Workshop on Geothermal Reservoir Engineering* (pp. 1-9). Stanford: Stanford University.

Younger, P. L. (2014). Missing a trick in geothermal exploration. *Nature Geoscience, 7*, 479-480.